Ground data confirm warming and drying are at a critical level for forest survival in western equatorial Africa

Emma R Bush Corresp., 1 , **Kathryn Jeffery** [1, 2] , **Nils Bunnefeld** [1] , **Caroline Tutin** [1] , **Ruth Musgrave** [3] , **Ghislain Moussavou** [4] , **Vianet Mihindou** [2, 5] , **Yadvinder Malhi** [6] , **David Lehmann** [1, 2] , **Josué Edzang Ndong** [2] , **Loïc Makaga** [2] , **Katharine A Abernethy** [1, 7]

[1] Faculty of Natural Sciences, University of Stirling, Stirling, United Kingdom

[2] Agence Nationale des Parcs Nationaux (ANPN), Libreville, Gabon

[3] Elephant Protection Initiative, London, UK

[4] Agence Gabonaise d'études et d'Observation Spatiale (AGEOS), Libreville, Gabon

[5] Ministère des Eaux et Forêts, charge de l'Environnement et du Développement Durable, Libreville, Gabon

[6] Environmental Change Institute, School of Geography and the Environment, University of Oxford, Oxford, United Kingdom

[7] Institut de Recherche en Écologie Tropicale, CENAREST, Libreville, Gabon

Corresponding Author: Emma R Bush
Email address: e.r.bush@stir.ac.uk

Background. The humid tropical forests of Central Africa influence weather worldwide and play a major role in the global carbon cycle. However they are also an ecological anomaly, with evergreen forests dominating the western equatorial region despite less than 2000mm total annual rainfall. Meteorological data for Central Africa are notoriously sparse and incomplete and there are substantial issues with satellite-derived data because of inability to ground-truth estimates and persistent cloudiness. Long-term climate observations are urgently needed to verify regional climate and vegetation models, shed light on the mechanisms that drive climatic variability and assess the viability of evergreen forests in equatorial Africa under future climate scenarios.

Methods. We have the rare opportunity to analyse a 34-year dataset of rainfall and temperature (and shorter periods of absolute humidity, wind speed, solar radiation and aerosol optical depth) from Lopé National Park, a long-term ecological research site in western equatorial Africa. We used linear mixed models and spectral analyses to assess seasonal and inter-annual variation, long-term trends and oceanic influences on local weather patterns.

Results. Lopé's weather is characterised by a light-deficient, cool, long dry season. Long-term climatic means have changed significantly over the last three decades, with warming occurring at a rate of 0.23°C per decade (minimum daily temperature) and drying at a rate of 50mm per decade (total annual rainfall). Inter-annual variability is highly influenced by sea surface temperatures of the major oceans. In El Niño years Lopé experiences both higher temperatures and less rainfall with increased contrast between wet and dry seasons. Lopé rainfall observations lend support for the role of the Atlantic cold tongue in "dry" models of climate change in the region.

Conclusions. Dry season cloud in western equatorial Africa plays a key role in reducing evaporative demand during seasonal drought and maintaining evergreen tropical forests despite relatively low annual rainfall. In the context of a rapidly warming and drying climate, urgent research is needed into the sensitivity of clouds to ocean temperatures and the viability of humid forests in this dry region should the clouds disappear.

PeerJ Preprints | https://doi.org/10.7287/peerj.preprints.27848v1 | CC BY 4.0 Open Access | rec: 10 Jul 2019, publ: 10 Jul 2019

Ground data confirm warming and drying are at a critical level for forest survival in western equatorial Africa

Emma R Bush [1], Kathryn J. Jeffery [1,2], Nils Bunnefeld [1], Caroline Tutin[1], Ruth Musgrave[3], Ghislain Moussavou[4], Vianet Mihindou [2,5], Yadvinder Malhi [6], David Lehmann [1,2], Josué Edzang Ndong[2], Loïc Makaga[2], Katharine A. Abernethy [1,7]

1 Faculty of Natural Sciences, University of Stirling, Stirling, UK
2 Agence Nationale des Parcs Nationaux (ANPN), Libreville, Gabon
3 Elephant Protection Initiative, London, UK.
4 L'Agence Gabonaise d'études et d'Observation Spatiale (AGEOS), Libreville, Gabon
5 Ministère des Eaux et Forêts, charge de l'Environnement et du Développement Durable, Libreville, Gabon
6 Environmental Change Institute, School of Geography and the Environment, University of Oxford, UK
7 Institut de Recherche en Écologie Tropicale, CENAREST, Libreville, Gabon

Corresponding Author:
Emma R. Bush,
Faculty of Natural Sciences, University of Stirling, Stirling, FK9 4LA, UK
Email address: e.r.bush@stir.ac.uk

PeerJ Preprints | https://doi.org/10.7287/peerj.preprints.27848v1 | CC BY 4.0 Open Access | rec: 10 Jul 2019, publ: 10 Jul 2019

Abstract

Background. The humid tropical forests of Central Africa influence weather worldwide and play a major role in the global carbon cycle. However they are also an ecological anomaly, with evergreen forests dominating the western equatorial region despite less than 2000mm total annual rainfall. Meteorological data for Central Africa are notoriously sparse and incomplete and there are substantial issues with satellite-derived data because of inability to ground-truth estimates and persistent cloudiness. Long-term climate observations are urgently needed to verify regional climate and vegetation models, shed light on the mechanisms that drive climatic variability and assess the viability of evergreen forests under future climate scenarios.

Methods. We have the rare opportunity to analyse a 34-year dataset of rainfall and temperature (and shorter periods of absolute humidity, wind speed, solar radiation and aerosol optical depth) from Lopé National Park, a long-term ecological research site in western equatorial Africa. We used linear mixed models and spectral analyses to assess seasonal and inter-annual variation, long-term trends and oceanic influences on local weather patterns.

Results. Lopé's weather is characterised by a light-deficient, cool, long dry season. Long-term climatic means have changed significantly over the last three decades, with warming occurring at a rate of 0.23°C per decade (minimum daily temperature) and drying at a rate of 50mm per decade (total annual rainfall). Inter-annual variability is highly influenced by sea surface temperatures of the major oceans. In El Niño years Lopé experiences both higher temperatures and less rainfall with increased contrast between wet and dry seasons. Lopé rainfall observations lend support for the role of the Atlantic cold tongue in "dry" models of climate change for the region.

Conclusions. Dry season cloud in western equatorial Africa plays a key role in reducing evaporative demand during seasonal drought and maintaining evergreen tropical forests despite relatively low annual rainfall. In the context of a rapidly warming and drying climate, urgent research is needed into the sensitivity of clouds to ocean temperatures and the viability of humid forests in this dry region should the clouds disappear.

Introduction

The humid forests of Central Africa make up 30% of the world's tropical forests (Malhi *et al.* 2013), are a major carbon store (Lewis *et al.* 2013) and influence weather globally (Bonan 2008; Washington *et al.* 2013). Most African evergreen tropical forests are found in the western equatorial region where total annual rainfall is less than 2000mm rainfall (Philippon et al. 2019). Evergreen forests can be maintained in this relatively dry region due to reduced water demand during seasonal drought associated with extreme cloudiness (Philippon et al. 2019). Long-term changes to climate and climatic variability in the region (James *et al.* 2013) are likely to have far-reaching impacts on the functioning of these evergreen tropical forests (Asefi-najafabady & Saatchi 2013; Zhou *et al.* 2014) with knock-on effects for the global carbon cycle (Mitchard 2018) and local human livelihoods (Niang et al., 2014).

However, evidence for changes in forest function linked to weather conditions in equatorial Africa is extremely rare, mainly due to missing long-term meteorological data. The number of rain gauge stations reporting data across Central Africa fell from a peak of more than 50 between 1950 and 1980 to fewer than ten in 2010 (Washington et al. 2013). This low density of observations and poor understanding of local landscape and climatic processes (Nicholson & Grist 2003) limits the accuracy of gridded observational data products (Asefi-najafabady & Saatchi 2013; Suggitt *et al.* 2017). Uncertainty is particularly high for rainfall patterns, which unlike temperature, are poorly conserved over space (Habib *et al.* 2001; Kidd *et al.* 2017).

Because of missing ground data, climate and ecological models rely heavily on satellites despite major issues with this data source also due to extreme cloudiness in the region and little opportunity for ground-truthing (Washington *et al.* 2013; Maidment *et al.* 2014; Wilson & Jetz 2016; Dommo *et al.* 2018). Empirical climate observations are urgently needed to verify regional climate and vegetation models and shed light on the mechanisms that drive seasonal and long-term climatic variability in tropical Africa (Guan *et al.* 2013; Abernethy *et al.* 2016).

We have the rare opportunity to analyse a 34-year record of rainfall and temperature (and shorter periods of humidity, wind speed, solar radiation and aerosol optical depth) from a long-term ecological research site in western equatorial Africa. These local weather data have not contributed to the regional climate products available and are able to act as an independent control. In this paper we briefly review the published literature on drivers of weather variability and long-term climate trends in western equatorial Africa (~6°S-5°N, 8°-18°E, covering

Cameroon, Republic of Congo, Central African Republic, Democratic Republic of Congo, Equatorial Guinea and Gabon). We then use our ground data to analyse seasonal, inter-annual and long-term weather patterns in this data-poor region with particular focus on rainfall for which uncertainty in regional products is high.

Seasonality

The climate of equatorial Africa is characterised by a bimodal rainfall pattern. Two rainy seasons occur each year coinciding with the boreal spring and autumn when the sun passes directly over the equator (March-May and October-November). Just 3% total annual rainfall falls during the major dry season, which extends from June to August/September (Balas et al. 2007). The primary influence on equatorial rainfall has historically been understood to be the Inter Tropical Convergence Zone (ITCZ), a band of clouds and high precipitation that migrates northwards and southwards over the equator following the sun (Nicholson 2018 and Fig. 1). However recent developments show the ITCZ to be a poor explanation of seasonal rainfall in Africa, with ITCZ-associated low-level convergence often found decoupled from the rain belt in western and central equatorial regions (Nicholson 2018). Improved mechanistic models of the seasonal evolution of atmospheric conditions in the region are urgently needed.

In western equatorial Africa the rainy seasons coincide with bright conditions. Convection clouds develop into storms late in the day or night leaving mainly clear skies during the daytime (Gond *et al.* 2013). By contrast the long dry season is when light is least available due to persistent low-lying cloud cover throughout the day (Philippon *et al.* 2019). The seasonal synchrony between light and moisture in western equatorial Africa is in contrast to the central Congo Basin and the neotropics where dry seasons tend to coincide with peak irradiance (Wright & Calderón 2018; Philippon *et al.* 2019). In western equatorial Africa the long dry season is also the coolest and windiest time of year (Munzimi et al. 2015; Tutin & Fernandez 1993; Preethi *et al.* 2015).

Oceanic influences

Large-scale patterns in sea surface temperatures (SSTs) are known to influence weather conditions across the tropics (Camberlin et al. 2001; Fig. 1). The El Niño Southern Oscillation (ENSO) refers to the state of the atmosphere and surface temperatures of the tropical Pacific Ocean. ENSO has a relatively straightforward, instantaneous effect on temperature throughout the African continent, with greater warming in El Niño years (Collins 2011). Central African rainfall is also strongly connected to SSTs (Otto *et al.* 2013), although interactions are complex and seasonally specific. In Table 1 we summarise six major studies of ocean influences on rainfall in western equatorial Africa (Todd & Washington 2004; Balas *et al.* 2007; Otto *et al.* 2013; Preethi *et al.* 2015 ; Nicholson & Dezfuli 2013; Dezfuli & Nicholson 2013). The main agreements between these studies are that (1) rainfall is below average from February to August in El Niño years (Camberlin *et al.* 2001; Todd & Washington 2004; Balas *et al.* 2007; Preethi *et al.* 2015; Nicholson & Dezfuli 2013), (2) rainfall positively correlates with the temperature of the Indian Ocean in January and February (Balas *et al.* 2007; Preethi *et al.* 2015) and (3) warm SSTs in the tropical South Atlantic enhance rainfall from April-September (Camberlin *et al.* 2001; Balas *et al.* 2007; Otto *et al.* 2013; Nicholson & Dezfuli 2013).

Long-term trends

There is high confidence in the evidence for warming over African land regions (Niang *et al.* 2014). Satellite estimates for tropical Africa show an annual mean temperature increase of 0.15°c per decade from 1979-2010 (Collins 2011). A recent multi-model ensemble shows that mean temperature for the whole continent is likely to continue to increase more than the global average especially in the long dry season (James & Washington 2013).

Tropical land areas globally have seen no overall change in precipitation over the last century, with a recent increase in precipitation (2003-2013) reversing a drying trend from the 1970s to the 1990s (Hartmann *et al.* 2013). Rainfall patterns are poorly conserved spatially and conflicting trends are detected within the western equatorial region of Africa. A regionalised long-term dataset for Africa constructed from historical records and rain gauge observations shows a sharp reduction in rainfall in the Cameroon region from the late 1960s until the present and a contrasting wetting trend in the Congo / Gabon region from 1980s until the present (Nicholson *et al.* 2018). However a higher resolution analysis of the same dataset shows that within central Gabon there has been a drying trend from the 1970s until 2000 and also reveals that there is no data available for this area for the last two decades (Nicholson *et al.* 2018). Flow data for the river Ogooué – the largest river in western equatorial Africa - indicates that runoff in the region declined from the 1960s until 2010 and that the flood peak has moved from May to April (Mahe *et al.* 2013). Land-cover change has been minimal in the watershed during this period

(Abernethy *et al.* 2016) and so it is likely that reduced rainfall has been the biggest influence on flow reduction.

Predictions of future rainfall vary widely across the African continent with high uncertainty in the direction of change centrally due to the sparse network of observations and poor understanding of local climate forcing (James & Washington 2013). Model projections mostly show no change or a weak wet signal in the central Congo Basin, and a dry signal in the western region in scenarios where warming is greater than 2°C (James et al. 2013). Models that support a drying trend in western equatorial Africa show strong associations with Atlantic and Indian (but not Pacific) SSTs. The construction of these dry models suggests that reductions in rainfall in Gabon and surrounding countries are likely to be caused by a northward displacement of the equatorial rain belt associated with the Atlantic cold tongue (Fig. 1B) and an eastward shift in convection caused by contrasts between Indian and Atlantic SSTs (James et al. 2013).

Humid evergreen forests currently dominate western equatorial Africa. Intense rainfall seasonality alongside a drying and warming climate would be expected to push this region towards drought-adapted deciduous ecosystems. However few meteorological data are available, especially in recent decades, to understand if the climatic trends described above are witnessed on the ground and how quickly are they progressing. Using our ground data from Lopé NP we ask: How fast is the region warming? Is the region drying and how quickly? And how do the oceans influence rainfall and temperature variability? Answers to these questions will be important to predict the viability of evergreen forest ecosystems under future climates.

Materials & Methods

Description of the study area and weather data recorded since 1984

The Station d'Études des Gorilles et Chimpanzées (SEGC) research station is located at the northern end of Lopé National Park, Gabon (-0.2N, 11.6E). The station sits in a tropical forest-savanna matrix, at an elevation of 280m and within 10.5 km of the river Ogooué. Ecological research activities including weather, plant and animal observations have taken place continuously at SEGC from 1984 until the present (>300 publications; 1984-2018).

Weather data have been recorded at Lopé using various types of equipment at two locations: a savanna site (the research station; 11.605E, -0.201N) and a forest site (800m from the research station and approximately 10m from the savanna/forest edge; 11.605E, -0.206N). From 1984 to the present, a manual rain gauge was placed at the savanna site (50cm above ground >5m from any tree or building) and used to record total daily rainfall at 8am each morning. There was a gap in data recording in 2013 and occasional missing days due to logistical constraints (e.g. availability of personnel). Since 1984 daily maximum and minimum temperatures and relative humidity were recorded using a manual thermometer and wet/dry bulb located at the forest site (1.5m aboveground under closed canopy), which was checked whenever field teams passed it or daily when logistics permitted. In 2002 all temperature recording at the forest site was transferred to continuous automatic units (ONSET HOBO® Data Loggers refhttps://www.onsetcomp.com/, these units also recorded relative humidity). At the same time temperature recording using the HOBO units also began in the savanna. Due to technical failures these units were replaced in 2006 with the original manual max/min thermometer in the forest and a digital max/min thermometer (Taylor 1441) in the savanna. These were in turn replaced by another type of automated unit (TinyTag Plus 2, Gemini Data Loggers https://www.geminidataloggers.com/data-loggers/tinytag-plus-2, some of which record both temperature and relative humidity). TinyTags were deployed in the forest from 2007 and in the savanna from 2008 and used until the present (with a gap at the forest site from mid-2015 to mid-2016 and intermittent recording throughout 2017 partly due to termite infestation). Two weather stations were installed in the savanna (sited near the research station, on a rock 4m from the ground) and collected data between 2012 and 2016. A Davis VantagePro2 (https://www.davisinstruments.com/solution/vantage-pro2/) was installed in January 2012 and recorded rainfall, temperature, relative humidity, pressure, wind speed and direction, UV index and solar radiation every 30 minutes for two years until the equipment was struck by lightning in January 2014. A SKYE MINIMET weather station (https://www.skyeinstruments.com/minimet-automatic-weather-station/) was installed at the same location in 2013 and collected temperature, relative humidity, wind speed and direction and solar radiation (and was also programmed to collect rainfall although this never worked). The SKYE unit ran intermittently until 2016 when the equipment was also damaged by lightning: data records between January 2014 and November 2014 were also lost. Finally, a sun photometer was installed at the research station in April 2014 and used to record aerosol optical depth up to the present as part of the NASA Aerosol Robotic Network (Aeronet; https://aeronet.gsfc.nasa.gov/; Holben et al. 1998).

Despite sustained effort, the remote and challenging environment at Lopé has led to a patchy weather data record. This situation has been exacerbated since the introduction of automated loggers, due to unreliable performance combined with difficulties and time delays in replacing or repairing malfunctioning equipment and respecting annual calibration schedules with manufacturers based in Europe or the USA. New equipment was often introduced out of necessity when previous equipment failed, precluding the opportunity of collecting simultaneous data for standardisation. Such problems have been experienced at many other field stations across Africa (Maidment *et al.* 2017). It was therefore necessary to select and standardise the Lopé data to reduce systematic biases between recording equipment. We summarise the data selection we undertook below and provide further detail in the accompanying Supplemental Information (Article S1 and Code S1). All Lopé data can be downloaded from the University of Stirling's DataSTORRE (http://hdl.handle.net/11667/133).

We constructed a long-term record of daily rainfall totals (1984-2018) by calibrating the two sources of data (rain gauge and weather station) using a simple linear model on simultaneous records and taking the mean value for days with multiple observations (12050 daily observations). Where possible we interpolated missing daily values (3% observations) using the ten-day running mean for the time series (resulting in 12419 daily observations), however 11 months spread over three calendar years remained incomplete. We used interpolated daily data to calculate total monthly and annual rainfall for the months and years with complete data (397 monthly observations and 31 years).

Temperature data were recorded using six different types of equipment across two sites (recorded in the forest from 1984 to 2018 and in the savanna from 2002 to 2018). We calculated mean daily maximum and minimum values at each site for each day in the time series with multiple observations and used this dataset to demonstrate temperature seasonality (7058 daily observations from the forest and 4878 daily observations from the savanna). To create a continuous time series for periodicity analyses we calculated mean monthly maximum and minimum daily temperatures for each month in the time series (excluding months with fewer than five observations) and filled gaps using the mean value for the corresponding calendar month from the whole time series (408 monthly observations from the forest site and 192 monthly observations from the savanna site).

Minimum daily temperature is recorded during the night and thus avoids errors associated with direct solar radiation (which we found to vary between our equipment, Article S1). We therefore chose to use minimum daily temperature only to assess trends and inter-annual variation. We constructed a long-term daily record combining minimum daily temperature data from both sites (8217 daily observations). We summarized this data to a monthly mean time series (371 monthly observations with 36 months excluded).

Finally we used shorter (and/or patchier) periods of data for relative humidity (2002-2018), solar radiation (2012-2016), wind speed (2012-2016) and aerosol optical depth (2014-2017) to assess seasonality and periodicity for these climate variables. We used night-time relative humidity records (6pm-6am) to avoid errors associated with direct solar radiation and converted to absolute humidity (g/m^3) using simultaneous temperature records within the R package *humidity* (Cai 2008). We extracted aerosol optical depth data at wavelengths relevant for photosynthetic activity (440, 500 and 675nm).

Gridded regional temperature datasets

Because of missing data and lack of simultaneous recording between temperature equipment at Lopé we also downloaded two widely used gridded regional data products with which to compare the Lopé data: daily minimum air temperature from the Gridded Berkeley Earth Surface Temperature Anomaly Field (1° resolution; Rohde *et al.* 2013) and monthly mean daily minimum temperature from the Climate Research Unit's Time-Series v4.01 of high-resolution gridded data (CRU TS4.01; 0.5° resolution; University of East Anglia Climatic Research Unit et al. 2017; Harris et al. 2014). Both were downloaded from http://climexp.knmi.nl/start.cgi for the grid-cell overlapping the SEGC location (0.2N, 11.6E).

Ocean Sea Surface Temperatures (SSTs)

We downloaded data for four oceanic SSTs from commonly used data sources: the Multivariate ENSO Index (MEI; Wolter & Timlin 1993; Wolter & Timlin 1998) sourced from the NOAA website (https://www.esrl.noaa.gov/psd/enso/mei/index.html), the Indian Ocean Dipole (IOD) Dipole Mode Index (Saji & Yamagata 2003) sourced from the NOAA website (https://www.esrl.noaa.gov/psd/gcos_wgsp/Timeseries/DMI/) and SST anomalies for the tropical north Atlantic (NATL, 5°–20°N, 60°–30°W) and the south equatorial Atlantic (SATL ,0°–20°S, 30°W–10°E) sourced from the NOAA National Weather Service Climate Prediction Center (http://www.cpc.ncep.noaa.gov/data/indices/). We rescaled all four SST indices by subtracting the mean and dividing by one standard deviation to allow direct comparison of modeled effect sizes. Positive values for MEI indicate El Niño conditions; positive values for NATL and SATL indicate warm SSTs in those regions while positive values for IOD indicate cool SSTs in South Eastern equatorial Indian Ocean and warm SSTs in the Western equatorial Indian Ocean.

Analyses

Seasonality

To describe the seasonality of each weather variable, we used empirical daily data to calculate the mean value for each day of the calendar year (DOY), the ten-day running mean of DOY and the mean for each calendar month. This allowed us to summarise the data while retaining fine-scale variation where available. To assess periodicity for each variable we used spectral analyses. First we created standardised time series by calculating the mean value for each month in the record, filling missing months using the mean value for the corresponding calendar month from the whole time series and standardizing by subtracting the mean and dividing by its standard deviation. We then computed the Fourier transform for each time series and inspected the spectra for peaks that represent strong regular cycles in the data (Bush et al. 2017).

Long-term trends

We assessed whether rainfall and minimum temperature have changed linearly over the observation period (1984-2018) within a linear regression framework. We fitted a generalized linear model (GLM, family = poisson) for total annual rainfall and a linear mixed model (LMM) for minimum daily temperature, accounting for both the distribution and hierarchical structure of the response data. To represent long-term change, we fitted models with Year (continuous, rescaled) as the predictor and compared these to intercept-only models, representing no long-term change, using AIC values. In all model comparisons we preferred simple models (few parameters) with lowest AIC (significantly different if delta AIC >2). We repeated the same procedure using LMMs for gridded data for Lopé from the daily Berkeley dataset and the monthly CRU dataset.

Next we investigated whether trends in rainfall and minimum temperature varied seasonally. Various seasonal definitions are used throughout the tropics, usually related to the annual rainfall cycle. We defined our seasons according to Lopé rainfall climatology where the long dry season extends into September, i.e. October-November (ON, the short rainy season), December-February (DJF, the short dry season), March-May (MAM, the long rainy season) and June-September (JJAS, the long dry season; Fig. 2A). We used daily rainfall and daily minimum temperature as response variables and fitted initial models (generalized linear mixed model, GLMM, for rainfall and LMM for temperature) including Year (continuous, rescaled), Season (factor with four levels as above) and their interaction as predictors to represent long-term change varying by season. We fitted subsequent models without the interaction term to represent long-term change not varying by season and compared the models using AIC values to test if the interaction improved the model. We modified the best models by temporarily removing the global intercept to estimate the magnitude of the trend for each season rather than comparing to the global intercept.

To account for the hierarchical structure of the data and to avoid pseudoreplication we included Year and DOY as random intercepts for all mixed models with daily response data (Lopé and Berkely minimum daily temperature Lopé daily rainfall) and Year and Month as random intercepts in the mixed model with monthly response data (CRU mean monthly minimum daily temperature). Inspection of the autocorrelation functions for total annual rainfall and the median autocorrelation functions for the daily and monthly temperature and rainfall datasets (autocorrelation calculated for each DOY or Month) showed no significant temporal autocorrelation. All models were fitted using the R package *lme4* (Bates et al. 2015) while autocorrelation functions for mixed models were calculated using the R package *itsadug* (van Rij 2017).

Periodicity over time

We used wavelet analyses to assess if and how periodicity varied over time for rainfall and temperature, explicitly taking account of the circular nature of the data (Adamowski *et al.* 2009). We computed the wavelet transform for the standardised monthly timeseries for each variable using the function *wt* from the R package *biwavelet* (Gouhier *et al.* 2018) and plotted the power (higher power denotes greater fidelity to a certain cycle), significance (a cycle is significant if >0.95, X^2 test) and cone of influence (denoting the unreliable region at the beginning and end of the time series due to edge effects). We then extracted the power of the biannual, annual and multiannual (mean of the 2-4 year periods) components to assess how these dominant cycles varied over time. We constrained the upper limit of the multiannual component to four years because lower frequency cycles were heavily influenced by edge effects.

Oceanic influences

We tested the seasonal influence of oceanic SSTs for the three major oceans hypothesized to influence weather in the Gabon region (Pacific: MEI, Indian Ocean: IOD and Atlantic Ocean: NATL and SATL) within a linear regression framework (GLMMs, family = poisson, for rainfall and LMMs for temperature). Using a monthly time series for each weather variable as the response variable, we fitted an initial model including each Oceanic Index (MEI, NATL, SATL and IOD), Season and the interactions between each Index and Season as predictor variables. For those weather variables that had previously shown to be changing linearly over time, we included Year (continuous, rescaled) and its interaction with Season as predictors. We modified these initial models by removing terms, starting with the interactions between each Oceanic Index and Season and ending with the Oceanic Index main effects, comparing models using AIC. As before, we refitted the best model without the global intercept to estimate the magnitude of the effect in each season rather than comparing each season effect to the global intercept. All models included Year and Month as random intercepts to account for pseudoreplication.

R code to accompany all analyses described above is made available in Supplemental Information (Code S1).

Results

Seasonality

Mean total annual rainfall at Lopé from 1984-2018 was 1466mm ± 201 sd. Rainfall in this period followed a biannual cycle (Fig. S1) with broad peaks in the rainy seasons (MAM and ON) when mean daily rainfall was always greater than 5mm (Fig. 2A). The long dry season (JJAS) was very consistent, with a 90-day period (mid-June to mid-September) in which the ten-day running mean was never greater than 1mm (Fig. 2A). The short dry season (DJF) by contrast was much less dry (ten-day running mean greater than 1mm) and more variable between years (Fig. 2A). Mean daily maximum and minimum temperatures at Lopé were 28.1°C ± 2.2 sd and 21.9°C ± 1.1 sd respectively at the forest site (1984-2018) and 31.6°C ± 2.9 sd and 22.0°C ± 1.2 sd at the savanna site (2002-2018). Daily temperature range was greater in the savanna than under the forest canopy (Fig. 2C and D). Maximum daily temperature in the forest showed strong annual and bi-annual cycles while in the savanna only the annual cycle appeared dominant (Fig. S1). The difference between the two sites occurred during the short dry season when temperatures were maintained in the savanna at similar levels to the rainy seasons (ten-day running mean always greater than 31.7°c from October to May in the savanna; Fig. 2C). In the forest, the highest peaks in maximum daily temperature occurred in April and September (mean monthly maximum daily temperatures were 29.5°c and 28.6°c respectively; Fig. 2D). Annual cycles dominated the minimum daily temperature record for both the forest and the savanna (Fig. S1). Minimum daily temperatures were relatively constant from September to June (~22.5°c) followed by a cool period during the long dry season reaching an annual trough in July (mean monthly minimum daily temperature is 20.6°c in both the savanna and forest; Fig. 2C and D). The forest was more humid than the savanna throughout the year (mean absolute humidity is 21.40 g/m^3 and 20.35 g/m^3 respectively; Fig. 2E and F). Humidity follows the same annual cycle in both locations (Fig. S1), dropping during the long dry season to reach a minima in August and increasing throughout the short rains (ON) to reach a plateau from January to May (Fig. 2E and F).

Both surface solar radiation and wind speed were dominated by annual cycles at Lopé (Fig. S1), with the long dry season coinciding with low irradiance (mean monthly solar radiation for July = 129.3 W/m2; Fig. 2G) and elevated wind speeds (mean monthly wind speeds for August and September are 1.3 m/s and 1.4m/s respectively; Fig. 2B). Aerosol optical depth cycled twice yearly (Fig. S1), elevated during the dry seasons and suppressed during the rainy seasons (Fig. 2H). In contrast to the solar radiation cycle, which reached its minima during the long dry season (JJAS), the strongest peak in aerosol optical depth occurred in the short dry season (mean monthly aerosol optical depth at 500nm for February = 0.97). Aerosol optical depth at 440 and 675nm wavelengths is similar to that at 500nm (Fig. S2).

Long-term trends

Total annual rainfall decreased by 50mm per decade, a change of -3.4% relative to mean annual rainfall for the time period (GLM, family = poisson, Estimate = -0.034 SE= 0.005, Z= -6.91, 95% Confidence Interval = (-0.044, -0.024); Table 2 and Fig. 3A). However the slope of the decline was seasonally dependent (Tables 3 and 4) with no change in daily rainfall in DJF and

ON and most rapid decline in JJAS (-0.26 mm per day per decade, equating to 23.6% of mean JJAS daily rainfall) followed by MAM (-0.19 mm per day per decade, equating to 3.1% of mean MAM rainfall).

Minimum daily temperature at Lopé increased at a rate of 0.23°c per decade, equivalent to 1.1% relative to mean minimum temperature for the time period (LMM, Estimate = 0.23; SE = 0.05; T = 5.2; 95% Confidence Interval = (0.14, 0.31); Table 2 and Fig. 3B). The rate of warming also varied by season (Tables 3 and 4) with minimum temperature increasing most quickly in ON and DJF (0.30°c and 0.29°c per decade respectively) and most slowly in JJAS (0.16°c per decade; Tables 2B and 3B)).

Berkeley minimum daily temperature for the interpolated Lopé grid square (1° resolution) increased at a rate of 0.16°c per decade (LMM, Estimate = 0.34, SE = 0.09, T = 3.9, 95% Confidence Interval = (0.17, 0.51) while the CRU interpolated record (0.5° resolution) increased by 0.19°c per decade (LMM, Estimate = 0.63 SE = 0.12, T = 5.4, 95% Confidence Interval = (0.40, 0.86)).

Periodicity over time

Wavelet analyses gave further indication of the nature of these changes. The dominant six-month cycle for rainfall was, on average, four times as powerful as the annual component and 66 times as powerful as the multi-annual component and remained significant for most of the time period (Fig. 3C). However the biannual cycle did lose power on three occasions (1996-97, 2004 and 2006; Fig. 3C). Over time, the biannual cycle in rainfall appeared to be losing power while the annual cycle was getting stronger (Fig. 3E).

The annual cycle for minimum temperature was, on average, three times as powerful as the biannual component and 23 times as powerful as the multi-annual component (Fig. 3F) and remained dominant throughout most of the time period with patches of low power at the end of the 1980s and between 2007 and 2010 (Fig. 3D). There were patches of high power in the multiannual component around 200. Both annual and semiannual components may be increasing in strength over time (Fig. 3F).

Oceanic influences

Rainfall was significantly correlated with SSTs of all three oceans while minimum temperature was significantly associated with the Pacific Ocean only (Table 5). The best model for rainfall incorporated all oceanic indices and each of their interactions with Season (Table 6 and Fig. 4A). El Niño conditions reduced rainfall in the months between June and February and increased rainfall in MAM (Fig. 4B). The El Niño effect was strongest in DJF and ON where a 1-point decrease in the ENSO index resulted in a predicted reduction of 32mm and 41mm rainfall per month respectively. By contrast in MAM a 1-point increase in the ENSO index led to a predicted increase of 6mm rainfall per month.

Warm North and South Atlantic SSTs coincided with greater than average rainfall in all seasons (all significantly different from zero apart from the effect of NATL in MAM; Fig. 4D and E). The South Atlantic had a greater impact on Lopé rainfall than the North Atlantic (size of the estimates; Table 6) and was especially strong in the months from March to September (Table 6 and Fig. 4D and E); A 1°C increase in the South Atlantic SST anomaly increased predicted monthly rainfall in MAM by 82mm and in JJAS by 17mm. Positive IOD modes coincided with enhanced rainfall in all seasons but was strongest (relative to the seasonal average) in JJAS (Table 6 and Fig. 4F) where a 1-point increase in the IOD resulted in an increase of 11mm to monthly predicted rainfall.

The best model for minimum daily temperature retained MEI (but not its interaction with season) as the only ocean influence on temperature (Tables 5 and 7 and Fig. 4A). El Niño conditions significantly increased minimum daily temperature in all seasons at Lopé (Fig. 4C) with a 1-point increase in the ENSO index resulting in a 0.13°c increase in mean annual minimum daily temperature.

There were weak positive correlations between IOD and MEI, IOD and NATL and between NATL and SATL (all <0.27; Fig. S3 and Fig. S4).

Discussion

Our results

Lopé weather has changed significantly over the last three decades, warming at a rate of 0.23°c per decade (minimum daily temperature) and drying at a rate of 50mm per decade (total annual rainfall). Both trends are seasonally dependent; significant warming occurred in all seasons, but was most rapid from October to February. Rainfall declined significantly between March and September, incorporating both the long rainy season and the long dry season. The drying trend at Lopé supports observations of reduced Ogooué river flow from March to September (Mahe et al.

2013) and precipitation declines evident from gridded gauge-data for the Gabon/Cameroon region (-1% total annual rainfall, 1968-1998; Malhi & Wright 2004). However, the Lopé total annual rainfall decline of -3.4% per decade exceeds the trend estimated from the regional gauge-data. While the strength of the biannual cycle in rainfall appears to be declining at Lopé along with the overall long-term trend, the annual component is getting more powerful. Declines in rainfall in the long dry season (June-September) but not the short dry season (December-February) are likely to be contributing to an increased contrast between the two dry seasons and enhancing an annual rainfall cycle.

The warming trend recorded at Lopé is greater than that estimated for the location over the same time period using the Berkeley and CRU gridded datasets (+0.16°C and +0.19°C respectively) and that identified using satellite data for mean annual temperature for all tropical Africa (0.15°c , 1979-2010; Collins 2011). However it is lower than the change estimated from gridded observational data (CRU) for mean annual temperature specifically for African tropical forests (+0.29°c per decade, 1976-1998; Malhi & Wright 2004). This latter analysis showed African tropical forests to be warming faster than those in both America and Asia (0.26 and 0.22°c per decade, respectively). While there remain issues with the Lopé temperature data record (lack of simultaneous recording to calibrate data recorded using different equipment), there is good evidence from supporting datasets and the literature that the warming trend observed at the site since 1984 is real. The slower warming trend in the already cool, long dry season is likely to account for the apparent increase in the power of the annual cycle for Lopé minimum temperature.

In addition to these directional trends in climatological averages, we found that interannual weather variability at our site is highly influenced by global weather patterns. Our analyses show that rainfall at Lopé is linked to the SST patterns of all three oceans while temperature is associated with the Pacific only. The SSTs of the North and South tropical Atlantic positively influence Lopé rainfall in all seasons with the influence being especially strong in the southern equatorial Atlantic from March to September. The association between Atlantic SSTs and rainfall is supported by other studies; Camberlin et al. (2001) found the Atlantic dipole (cool temperatures in the North Atlantic and warm temperatures in the South Tropical Atlantic) to be associated with higher than average rainfall in March-May, while Balas et al. (2007) found positive temperature anomalies in the southern equatorial Atlantic (especially the Benguela coast) to enhance rainfall in the long dry season. In another study, warm southern Atlantic anomalies were shown to correlate positively with rainfall in both dry seasons (Otto *et al.* 2013). South tropical Atlantic SSTs and circulation patterns have been an important influence on Congo Basin precipitation for the past 20,000 years (Schefuss *et al.* 2005).

Lopé rainfall is positively correlated with ENSO from March to May and negatively correlated from June to February, influencing the rainfall contrast between seasons. In La Niña years, rainfall is above average in the short dry season (December-February), making it more similar to the March-May rainy season (where rainfall is reduced under the same conditions). In El Niño years, rainfall is below average from December to February increasing the contrast between the short dry season and the rainy seasons, which are also more similar to each other at these times (Fig. 4B). While these findings support the conclusion that ENSO influences rainfall in the region, there are disagreements between our study and others. Among the major studies summarized in Table 1 negative associations were shown between ENSO and western equatorial African rainfall in all seasons. While we observed reduced rainfall at Lopé in El Niño years from June to February, we found a positive influence of ENSO on rainfall in March-May. Finally, we showed that positive dipole modes for the Indian Ocean (above average SSTs along the east African coast) are associated with increased rainfall in all seasons at Lopé. Published data show contrasting results, with reduced rainfall associated with positive IOD modes in both dry and rainy seasons (Dezfuli & Nicholson 2013; Nicholson & Dezfuli 2013; Otto *et al.* 2013). Overall, our work supports the idea that the drivers of rainfall variability in western equatorial Africa are highly complex, with strong local and seasonal forcing from the major oceans. Land topography (e.g. the highlands of Gabon, Cameroon and eastern Africa) is also likely to be a major influence on highly localised expressions of rainfall and rainfall variability in the region (Balas *et al.* 2007; Dezfuli *et al.* 2015).

Model projections of future rainfall in western equatorial Africa cover a broad spectrum and as a result, averaged model trends are close to zero. Those models that predict drying in the region do so due to a northward shift of the rainbelt, related to cool SSTs in the Gulf of Guinea in in all seasons, but most markedly in March-May (the Atlantic cold tongue; James et al. 2013). We found strong reductions in rainfall in these months associated with a cool southern equatorial Atlantic (0°- 20°S) and thus our data provide some support for the mechanisms behind these "dry" models.

We found that El Niño conditions are associated with above average minimum temperatures at Lopé from December to May; a result supported by a continent-wide study showing increased warming in El Niño years throughout Africa (Collins 2011). As the long-term trend in minimum temperature was retained alongside ENSO in our final model, it is likely that the El Niño effect is in addition to, and not the main influence on, long-term warming in the region (as in Collins 2011). The Atlantic and Indian Oceans had no significant effects on temperature at Lopé once the general warming trend was accounted for in our model, meaning that while both Lopé and the Atlantic oceans are warming, we find no evidence that one causes the other above and beyond the established global trend. The strong association between ENSO and Lopé minimum temperature is likely to account for the periodicity evident in the wavelet transform at ENSO scales (two to eight-year window).

Data quality and availability

One of the major issues with climate analyses in central Africa is the already limited and declining amount of publicly available data from weather stations in the region: The nearest weather stations to Lopé listed on the Global Historical Climatology Network (GCHN) Daily Database (Menne et al. 2012) are between 136 and 185km away and there are no public data available since 1980. The World Meteorological Organisation has a minimum recommended density of weather stations eight times higher than the modern density of weather stations in Africa (Collins 2011). This lack of data has a direct impact on the quality of gridded climate data products (Suggitt et al. 2017) and leads to an inability to calculate daily climatic indices for the extremes (Niang *et al.* 2014). Gabon is also one of the cloudiest places on earth (http://www.acgeospatial.co.uk/the-cloudiest-place/) which leads to large uncertainties in satellite estimates, with some satellite algorithms overestimating rainfall in the region by at least a factor of two (Balas *et al.* 2007). Finally, poor correlation between Central African rainfall and neighboring regions, as well as variability between individual stations, suggests much local influence and further confounds the challenges of sparse data (Balas *et al.* 2007).

The importance of maintaining long-term study sites and improving the quality and type of weather measurements in the region has been known for some time (Clark 2007). However, the region is remote and there are many financial, logistical and political challenges to face when servicing field stations. One such issue is that western equatorial Afria has the highest frequency of lightning strike in the world (Balas *et al.* 2007) leading to difficulties and great expense maintaining equipment. Lightning damage is an issue we regularly confront at Lopé and has led to major gaps in our data record. While automatic continuous measurements can provide vast amounts of detailed data relevant for ecological studies they are also inherently more susceptible to technical failures that need expert fixes. In our experience, data gaps are more likely to go unnoticed with automatic data collection and so while we welcome new automatic methods, we recommend maintaining long-term manual records alongside for consistency.

Conclusions

The long-term Lopé weather record has not previously been made public and is of high value in such a data poor region. Our results support regional analyses of climatic seasonality, long-term warming and the influences of the oceans on temperature and rainfall variability. However there are some surprises; warming has occurred more rapidly than the regional products suggest and while there remains much uncertainty as to the direction of precipitation change in the wider region, reduced rainfall over the last three decades at Lopé is in agreement with drying trends evident from less recent observational data for western equatorial Africa. The influence of the Atlantic cold tongue on rainfall at Lopé lends support to the mechanisms behind "dry" models for future rainfall in the region.

Our analysis further serves to emphasise the ecological importance of the long dry season in western equatorial Africa; three-four months of dry (almost no rainfall for 90 consecutive days), cool (mean maximum daily temperature is 2.5°C lower in July compared to April) and windy conditions with low humidity and limited light availability. Such a defined season poses specific challenges to the biota and is likely to act as a temporal marker for ecological events, similar to a winter event in temperate regions. The long dry season is likely to be an unfavourable period for photosynthesis and for most reproductive events that require high energy and moisture availability. The response of the plant community to this recurrent and predictable seasonal drought could be used to estimate their long-term response to drying over multi-annual time scales (Detto *et al.* 2018).

With a climatic regime delivering less than 1500mm per year, Lopé is an anomalously dry region for the persistence of evergreen tropical forests (Reich 1995). Reduced evaporative demand during the cloudy, light-deficient long dry season is likely to be the major factor facilitating persistence of evergreen forests (Philippon 2019). In the context of further drying and warming, it is essential that we understand the sensitivity of this seasonal cloudiness to ocean temperatures, and the viability of forest in this dry region should the clouds disappear.

Acknowledgements

We acknowledge significant periods of independent data collection undertaken by Richard Parnell, Edmond Dimoto and Lee White. Permission to conduct this research in Gabon was granted by the CIRMF Scientific Council and the Ministry of Water and Forests (1986 – 2010), and by ANPN and the National Centre for Research in Science and Technology (CENAREST; 2010 - present).

References

Abernethy, K., Maisels, F. & White, L.J.T. (2016). Environmental Issues in Central Africa. *Annual Review of Environment and Resources*, **41**, 1–33.

Adamowski, K., Prokoph, A. & Adamowski, J. (2009). Development of a new method of wavelet aided trend detection and estimation. *Hydrological Processes*, **23**, 2686–2696.

Asefi-najafabady, S. & Saatchi, S. (2013). Response of African humid tropical forests to recent rainfall anomalies. *Philosophical transactions of the Royal Society of London. Series B, Biological sciences*, **368**, 20120306,.

Balas, N., Nicholson, S.E. & Klotter, D. (2007). The relationship of rainfall variability in West Central Africa to sea-surface temperature fluctuations. *International Journal of Climatology*, **27**, 1335–1349.

Barlow, J., França, F., Gardner, T.A., Hicks, C.C., Lennox, G.D., Berenguer, E., Castello, L., Economo, E.P., Ferreira, J., Guénard, B., Gontijo Leal, C., Isaac, V., Lees, A.C., Parr, C.L., Wilson, S.K., Young, P.J. & Graham, N.A.J. (2018). The future of hyperdiverse tropical ecosystems. *Nature*, **559**, 517–526.

Bates, D., Maechler, M., Bolker, B. and Walker, S. (2015). Fitting Linear Mixed-Effects Models Using lme4. Journal of Statistical Software, 67(1), 1-48. doi:10.18637/jss.v067.i01.

Behera, S., Brandt, P. & Reverdin, G. (2013). The tropical ocean circulation and dynamics. *International Geophysics vol. 103*, pp. 385–412. Academic Press.

Bloomfield, P. (2000). *Fourier analysis of time series: an introduction*. John Wiley & Sons.

Bonan, G.B. (2008). Forests and climate change: forcings, feedbacks, and the climate benefits of

forests. *Science (New York, N.Y.)*, **320**, 1444–1449.
Borchert, R., Renner, S.S., Calle, Z., Havarrete, D., Tye, A., Gautier, L., Spichiger, R. & Von Hildebrand, P. (2005). Photoperiodic induction of synchronous flowering near the Equator. *Nature*, **433**, 627–629.
Bush, E.R., Abernethy, K.A., Jeffery, K., Tutin, C., White, L., Dimoto, E., Dikangadissi, J.T., Jump, A.S. & Bunnefeld, N. (2017). Fourier analysis to detect phenological cycles using tropical field data and simulations. *Methods in Ecology and Evolution*, **8**, 530–540.
Cai, J., 2018. humidity: Calculate Water Vapor Measures from Temperature and Dew Point. R package version 0.1.4. Available at: https://github.com/caijun/humidity.
Camberlin, P., Janicot, S. & Poccard, I. (2001). Seasonality and atmospheric dynamics of the teleconnection between African rainfall and tropical sea-surface temperature: Atlantic vs. ENSO. *International Journal of Climatology*, **21**, 973–1005.
Clark, D.A. (2007). Detecting Tropical Forests ' Responses to Global Climatic and Atmospheric Change : Current Challenges and a Way Forward. **39**, 4–19.
Collins, J.M. (2011). Temperature variability over Africa. *Journal of Climate*, **24**, 3649–3666.
Cusack, D., Karpman, J., Ashdown, D., Cao, Q., Ciochina, M., Halternman, S., Lydon, S. & Neupane, A. (2013). Global change effects on humid tropical forests: Evidence for biogeochemical and biodiversity shifts at an ecosystem scale. *Review of Geophysics*, **54**, 523–610.
Detto, M., Wright, S.J., Calderón, O. & Muller-landau, H.C. (2018). Resource acquisition and reproductive strategies of tropical forest in response to the El Niño–Southern Oscillation. *Nature Communications*, **9**, 913.
Dezfuli, A.K. & Nicholson, S.E. (2013). The Relationship of Rainfall Variability in Western Equatorial Africa to the Tropical Oceans and Atmospheric Circulation . Part II : The Boreal Autumn. *Journal of Climate*, **26**, 66–84.
Nicholson, S.E. (2018). The ITCZ and the seasonal cycle over equatorial Africa. *Bulletin of the American Meteorological Society*, **99**, 337–348.
Nicholson, S.E. & Dezfuli, A.K. (2013). The Relationship of Rainfall Variability in Western Equatorial Africa to the Tropical Oceans and Atmospheric Circulation . Part I : The Boreal Spring. *Journal of Climate*, **26**.
Nicholson, S.E., Funk, C. & Fink, A.H. (2018). Rainfall over the African continent from the 19th

through the 21st century. *Global and Planetary Change*, **165**, 114–127.

Otto, F.E.L., Jones, R.G., Halladay, K. & Allen, M.R. (2013). Attribution of changes in precipitation patterns in African rainforests. *Philosophical transactions of the Royal Society of London. Series B, Biological sciences*, **368**, 20120299.

Dezfuli, A.K., Zaitchik, B.F. & Gnanadesikan, A. (2015). Regional atmospheric circulation and rainfall variability in south equatorial Africa. *Journal of Climate*, **28**, 809–818.

Dommo, A., Philippon, N., Vondou, D.A., Seze, G. & Eastman, R. (2018). The June – September Low Cloud Cover in Western Central Africa : Mean Spatial Distribution and Diurnal Evolution. **31**, 9585–9603.

Farnsworth, A., White, E., Williams, C.J.R., Black, E. & Kniveton, R. (2011). Understanding the Large Scale Driving Mechanisms of Rainfall Variability over Central Africa. *African Climate and Climate Change*, pp. 101–122. Springer, Dordecht.

Gond, V., Fayolle, A., Pennec, A., Cornu, G., Mayaux, P., Doumenge, C., Fauvet, N., Gourlet-fleury, S., B, P.T.R.S. & Camberlin, P. (2013). Vegetation structure and greenness in Central Africa from Modis multi-temporal data. *Philosophical transactions of the Royal Society of London. Series B, Biological sciences*, **368**, 20120309.

Gouhier, T.C., Grinsted, A. & Simko, V. (2018). R package biwavelet: Conduct Univariate and Bivariate Wavelet Analyses.

Guan, K., Wolf, A., Medvigy, D., Caylor, K., Pan, M. & Wood, E.F. (2013). Seasonal coupling of canopy structure and function in African tropical forests and its environmental controls. *Ecosphere*, **4**, 1–21.

Habib, E., Krajewski, W.F. & Ciach, G.J. (2001). Estimation of Rainfall Interstation Correlation. *Journal of Hydrometeorology*, **2**, 621–629.

Harris, I., Jones, P.D., Osborn, T.J. & Lister, D.H. (2014). Updated high-resolution grids of monthly climatic observations - the CRU TS3.10 Dataset. *International Journal of Climatology*, **34**, 623–642.

Hartmann, D.L., Klein Tank, A.M.G., Rusticucci, M., Alexander, L. V., Brönnimann, S., Charabi, Y.A.R., Dentener, F.J., Dlugokencky, E.J., Easterling, D.R., Kaplan, A., Soden, B.J., Thorne, P.W., Wild, M. & Zhai, P. (2013). Observations: Atmosphere and surface. *Climate Change 2013 the Physical Science Basis: Working Group I Contribution to the Fifth Assessment Report of the Intergovernmental Panel on Climate Change* (eds T.F.

Stocker, D. Qin, G.-K. Plattner, M. Tignor, S.K. Allen, J. Boschung, A. Nauels, Y. Xia, V. Bex & P.M. Midgley), pp. 159–254. Cambridge University Press, Cambridge, United Kingdom and New York, NY, USA.

Helder, C., Sousa, R. De, Hilker, T., Waring, R., Moura, Y.M. De & Lyapustin, A. (2017). Progress in Remote Sensing of Photosynthetic Activity over the Amazon Basin. *Remote Sensing*, **9**, 148.

Holben, B.N., Eck, T.F., Slutsker, I., Tanré, D., Buis, J.P., Setzer, A., Vermote, E., Reagan, J.A., Kaufman, Y.J., Nakajima, T., Lavenu, F., Jankowiak, I. & Smirnov, A. (1998). AERONET—A Federated Instrument Network and Data Archive for Aerosol Characterization. *Remote Sensing of Environment*, **66**, 1–16.

James, R. & Washington, R. (2013). Changes in African temperature and precipitation associated with degrees of global warming. *Climatic Change*, **117**, 859–872.

James, R., Washington, R. & Rowell, D.P. (2013). Implications of global warming for the climate of African rainforests. *Philosophical Transactions of the Royal Society B: Biological Sciences*, **368**, 20120298,.

Kidd, C., Becker, A., Huffman, G.J., Muller, C.L., Joe, P., Skofronick-Jackson, G. & Kirschbaum, D.B. (2017). So, how much of the Earth's surface is covered by rain gauges? *Bulletin of the American Meteorological Society*, **98**, 69–78.

Kothe, S., Pfeifroth, U., Cremer, R., Trentmann, J. & Hollmann, R. (2017). A Satellite-Based Sunshine Duration Climate Data Record for Europe and Africa. *Remote Sensing*, **9**, 429.

Laraque, A., Mahé, G., Orange, D. & Marieu, B. (2001). Spatiotemporal variations in hydrological regimes within Central Africa during the twentieth century. *Journal of Hydrology,* **245**, **1–4,** 104–117.

Lewis, S.L., Sonké, B., Sunderland, T., Begne, S.K., Lopez-gonzalez, G., Heijden, G.M.F. Van Der, Phillips, O.L., Affum-baffoe, K., Baker, T.R., Banin, L., Bastin, J., Beeckman, H., Boeckx, P., Bogaert, J., Cannière, C. De, Clark, C.J., Collins, M., Djagbletey, G., Djuikouo, M.N.K., Doucet, J., Ewango, C.E.N., Fauset, S., Feldpausch, T.R., Ernest, G., Gillet, J., Hamilton, A.C., Harris, D.J., Hart, T.B., Haulleville, T. De, Hladik, A., Hufkens, K., Huygens, D., Jeanmart, P., Jeffery, K.J., Leal, M.E., Lloyd, J., Lovett, J.C., Makana, J., Malhi, Y., Andrew, R., Ojo, L., Peh, K.S., Pickavance, G., Poulsen, J.R., Reitsma, J.M., Sheil, D., Simo, M., Steppe, K., Taedoumg, H.E., Talbot, J., James, R.D., Taylor, D.,

PeerJ Preprints | https://doi.org/10.7287/peerj.preprints.27848v1 | CC BY 4.0 Open Access | rec: 10 Jul 2019, publ: 10 Jul 2019

Thomas, S.C., Toirambe, B., Verbeeck, H., Vleminckx, J., Lee, J., White, T., Willcock, S., Woell, H., Zemagho, L., B, P.T.R.S., Sonke, B., Poulsen, R. & Thomas, C. (2013). Above-ground biomass and structure of 260 African tropical forests. *Philosophical transactions of the Royal Society of London. Series B, Biological sciences*, **368**, 20120295.

Mahe, G., Lienou, G., Descroix, L., Bamba, F., Paturel, J.E., Laraque, A., Meddi, M., Habaieb, H., Adeaga, O., Dieulin, C., Chahnez Kotti, F. & Khomsi, K. (2013). The rivers of Africa: Witness of climate change and human impact on the environment. *Hydrological Processes*, **27**, 2105–2114.

Maidment, R.I., Allan, R.P. & Black, E. (2015). Recent observed and simulated changes in precipitation over Africa. *Geophysical Research Letters*, **42**, 8155–8164.

Maidment, R.I., Grimes, D., Allan, R.P., Tarnavsky, E., Stringer, M., Hewison, T., Roebeling, R. & Black, E. (2014). The 30-year TAMSAT African Rainfall Climatology And Time-series (TARCAT) Dataset. *Journal of Geophysical Research: Atmospheres*, **119.18**, 10–619.

Maidment, R.I., Grimes, D., Black, E., Tarnavsky, E., Young, M., Greatrex, H., Allan, R.P., Stein, T., Nkonde, E., Senkunda, S. & Alcántara, E.M.U. (2017). A new, long-term daily satellite-based rainfall dataset for operational monitoring in Africa. *Scientific Data*, **4**, 1–19.

Malhi, Y., Adu-bredu, S., Asare, R.A., Lewis, S.L., Mayaux, P. & B, P.T.R.S. (2013). The past, present and future of Africa's rainforests. *Philosophical transactions of the Royal Society of London. Series B, Biological sciences*, **368**, 20120293.

Malhi, Y. & Wright, J. (2004). Spatial patterns and recent trends in the climate of tropical rainforest regions. *Philosophical Transactions of the Royal Society B: Biological Sciences*, **359**, 311–329.

Menne, M.J., Durre, I., Vose, R.S., Gleason, B.E. & Houston, T.G. (2012). An Overview of the Global Historical Climatology Network-Daily Database. *Journal of Atmospheric and Oceanic Technology*, **29**, 897–910.

Mitchard, E.T.A. (2018). The tropical forest carbon cycle and climate change. *Nature*, **559**, 527–534.

Munzimi, Y., Hansen, M., Adusei, B. & Senay, G. (2015). Characterizing Congo Basin Rainfall and Climate Using Tropical Rainfall Measuring Mission (TRMM) Satellite Data and Limited Rain Gauge Ground Observations. *Journal of Applied Metereology and Climatology*, **54**, 541–555.

Nagai, S., Ichie, T., Yoneyama, A., Kobayashi, H., Inoue, T., Ishii, R., Suzuki, R. & Itioka, T. (2016). Usability of time-lapse digital camera images to detect characteristics of tree phenology in a tropical rainforest. *Ecological Informatics*, **32**, 91–106.

National Weather Service. (2018). Inter-Tropical Convergence Zone. *Jet Stream - An Online School for Weather*. URL https://www.weather.gov/jetstream/itcz [accessed 3 December 2018]

Niang, I., Ruppel, O.C., Abdrabo, M.A., Essel, A., Lennard, C., Padgham, J. & Urquhart, P. (2014). Africa. *Climate Change 2014: Impacts, Adaptation and Vulnerability - Contributions of the Working Group II to the Fifth Assessment Report of the Intergovernmental Panel on Climate Change.* (eds V.R. Barros, C.B. Field, D.J. Dokken, M.D. Mastrandrea, K.J. Mach, T.E. Bilir, M. Chatterjee, K.L. Ebi, Y.O. Estrada, R.C. Genova, B. Girma, E.S. Kissel, A.N. Levy, S. MacCracken, P.R. Mastrandrea & L.L. White), pp. 1199–1265. Cambirgde University Press, Cambirgde, UK and New York, NY, USA.

Nicholson, S.E. (2018). The ITCZ and the seasonal cycle over equatorial Africa. *Bulletin of the American Meteorological Society*, **99**, 337–348.

Nicholson, S.E. & Dezfuli, A.K. (2013). The Relationship of Rainfall Variability in Western Equatorial Africa to the Tropical Oceans and Atmospheric Circulation . Part I : The Boreal Spring. *Journal of Climate*, **26**.

Nicholson, S.E., Funk, C. & Fink, A.H. (2018). Rainfall over the African continent from the 19th through the 21st century. *Global and Planetary Change*, **165**, 114–127.

Nicholson, S.E. & Grist, J.P. (2003). The seasonal evolution of the atmospheric circulation over West Africa and equatorial Africa. *Journal of Climate*, **16**, 1013–1030.

NOAA. (2018). U.S. Daily Climate Normals (1981-2010). *National Centers for Environmental Information*. URL https://data.nodc.noaa.gov/cgi-bin/iso?id=gov.noaa.ncdc:C00823 [accessed 26 November 2018]

Otto, F.E.L., Jones, R.G., Halladay, K. & Allen, M.R. (2013). Attribution of changes in precipitation patterns in African rainforests. *Philosophical transactions of the Royal Society of London. Series B, Biological sciences*, **368**, 20120299.

Philippon, N., Cornu, G., Monteil, L., Gond, V., Moron, V., Pergaud, J., Sèze, G., Bigot, S., Camberlin, P., Doumenge, C., Fayolle, A. & Ngomanda, A. (2019). The light-deficient climates of western Central African evergreen forests. *Environmental Research Letters*, **14**, 34007.

Preethi, B., Sabin, T.P., AdeDay of Yearin, J.A. & Ashok, K. (2015). Impacts of the ENSO Modoki and other tropical indo-pacific climate-drivers on African rainfall. *Scientific Reports*, **5**, 1–15.

Reich, P.B. (1995). Phenology of tropical forests: patterns, causes, and consequences. *Canadian Journal of Botany*, **73**, 164–174.

Rohde, R., Muller, R.A., Jacobsen, R., Muller, E., Perlmutter, S., Rosenfeld, A., Wurtele, J., Groom, D. & Wickham, C. (2013). A new estimate of the average Earth surface land temperature spanning 1753 to 2011. *Geoinfor Geostat Overview 1*, **7**, 2.

Saji, N.H. & Yamagata, T. (2003). Possible impacts of Indian Ocean dipole mode events on global climate. *Climate Research*, **25**, 151–169.

Sakai, S. (2001). Phenological diversity in tropical forests. *Population Ecology*, **43**, 77–86.

van Schaik, C.P., Terborgh, J.W. & Wright, J.S. (1993). The phenology of tropical forests: Adaptive significance and consequences for primary consumers. *Annual Review of Ecology and Systematics*, **24**, 353–377.

Schefuss, E., Schouten, S. & Schneider, R.R. (2005). Climatic controls on central African hydrology during the past 20 , 000 years. *Nature*, **437**, 1003–1006.

Suggitt, A.J., Platts, P.J., Barata, I.M., Bennie, J.J., Burgess, M.D., Bystriakova, N., Duffield, S., Ewing, S.R., Gillingham, P.K., Harper, A.B., Hartley, A.J., Hemming, D.L., Maclean, I.M.D., Maltby, K., Marshall, H.H., Morecroft, M.D., Pearce-Higgins, J.W., Pearce-Kelly, P., Phillimore, A.B., Price, J.T., Pyke, A., Stewart, J.E., Warren, R. & Hill, J.K. (2017). Conducting robust ecological analyses with climate data. *Oikos*, **126**, 1533–1541.

Suzuki, T. (2011). Seasonal variation of the ITCZ and its characteristics over central Africa. *Theoretical and Applied Climatology*, **103**, 39–60.

Todd, M.C. & Washington, R. (2004). Climate variability in central equatorial Africa: Influence from the Atlantic sector. *Geophysical Research Letters*, **31**, 1–4.

Tutin, C.E.G. & Fernandez, M. (1993). Relationships between minimum temperature and fruit production in some tropical forest trees in Gabon. *Journal of Tropical Ecology*, **9**, 241–248.

University of East Anglia Climatic Research Unit, Harris, I.C.. & Jones, P.D. (2017). *CRU TS4.01: Climatic Research Unit (CRU) Time-Series (TS) version 4.01 of high-resolution* *gridded data of month-by-month variation in climate (Jan. 1901- Dec. 2016).*

van Rij J, Wieling M, Baayen R, van Rijn H (2017). “itsadug: Interpreting Time Series.

and Autocorrelated Data Using GAMMs.” R package version 2.3.Washington, R., James, R., Pearce, H., Pokam, W.M. & Moufouma-Okia, W. (2013). Congo Basin rainfall climatology: can we believe the climate models? *Philosophical transactions of the Royal Society of London. Series B, Biological sciences*, **368**, 20120296.

Willis, K.J., Bennett, K.D., Burrough, S.L., Macias-Fauria, M. & Tovar, C. (2013). Determining the response of African biota to climate change : using the past to model the future. *Philosophical transactions of the royal society*, **368**, 20120491.

Wilson, A.M. & Jetz, W. (2016). Remotely Sensed High-Resolution Global Cloud Dynamics for Predicting Ecosystem and Biodiversity Distributions. *PLOS Biology*, **14**, e1002415.

Wolter, K. (2018). Multivariate ENSO Index (MEI). URL https://www.esrl.noaa.gov/psd/enso/mei/ [accessed 24 July 2018]

Wolter, K. & Timlin, M.S. (1998). Measuring the strength of ENSO events: How does 1997/98 rank? *Weather*, **53**, 315–324.

Wolter, K. & Timlin, M.S. (1993). Monitoring ENSO in COADS with a seasonally adjusted principal component index. *Proc. of the 17th Climate Diagnostics Workshop*, pp. 52–57. Norman, OK, NOAA/NMC/CAC, NSSL, Oklahoma Clim. Survey, CIMMS and the School of Meteor., Univ. of Oklahoma.

Wright, S. (1996). Phenological responses to seasonality in tropical forest plants. *Tropical forest plant ecophysiology*, pp. 440–460. Springer, Boston, MA.

Wright, S.J. & Calderón, O. (2018). Solar irradiance as the proximate cue for flowering in a tropical moist forest. *Biotropica*, **50**, 374–383.

Zhang, Y., Tan, Z., Song, Q., Yu, G. & Sun, X. (2010). Respiration controls the unexpected seasonal pattern of carbon flux in an Asian tropical rain forest. *Atmospheric Environment*, **44**, 3886–3893.

Zhou, L., Tian, Y., Myneni, R.B., Ciais, P., Saatchi, S., Liu, Y.Y., Piao, S., Chen, H., Vermote, E.F., Song, C. & Hwang, T. (2014). Widespread decline of Congo rainforest greenness in the past decade. *Nature*, **508**, 86–90.

Figure 1(on next page)

Global climatic influences on western equatorial Africa

(A) The forested region of central Africa is indicated by a layer of green pixels (>30% tree cover in 2010 from Hansen et al. 2013). The Northern (July) and Southern limits (January) of the Inter Tropical Convergence Zone (ITCZ) are drawn from Barlow et al. (2018). The blue zones indicate patterns in oceanic sea surface temperatures (SSTs) known to influence weather in western Central Africa: the Pacific Ocean El Niño Southern Oscillation (ENSO); North and South Tropical Atlantic SSTs (NATL and SATL) and the Indian Ocean Dipole (IOD). In conventional El Niño years the tropical Eastern Pacific is abnormally warm, in El Niño Modoki the warming occurs in the central Pacific. The IOD is the difference between SSTs of the western and eastern tropical Indian Ocean. (B) The limits of western equatorial Africa as defined in this paper are indicated by the grey rectangle (including the humid forests of Gabon, Equatorial Guinea, Cameroon and the Republic of Congo). We also show the location of the seasonal Atlantic cold tongue, a pool of cool surface water that develops in the eastern tropical Atlantic during the boreal summer (Tokinaga & Xie 2011). Tree cover data are available from http://earthenginepartners.appspot.com/science-2013-global-forest. The world map was created by Layerace at Freepik.com.

PeerJ Preprints | https://doi.org/10.7287/peerj.preprints.27848v1 | CC BY 4.0 Open Access | rec: 10 Jul 2019, publ: 10 Jul 2019

Figure 2(on next page)

Seasonal weather variability at Lopé NP, Gabon.

Mean seasonality for daily rainfall (1984-2018), maximum and minimum daily temperature (1984-2017), relative humidity (2007-2015), surface solar radiation (2012-2016), wind speed (2012-2016) and aerosol optical depth at 500nm (2014-2017). The thin grey lines indicate the mean values for each day of the calendar year (DOY). The thin black lines indicate the seven-day running means of DOY and the thick black lines indicate the monthly means. Vertical dotted lines indicate the alternating rainy and dry seasons.

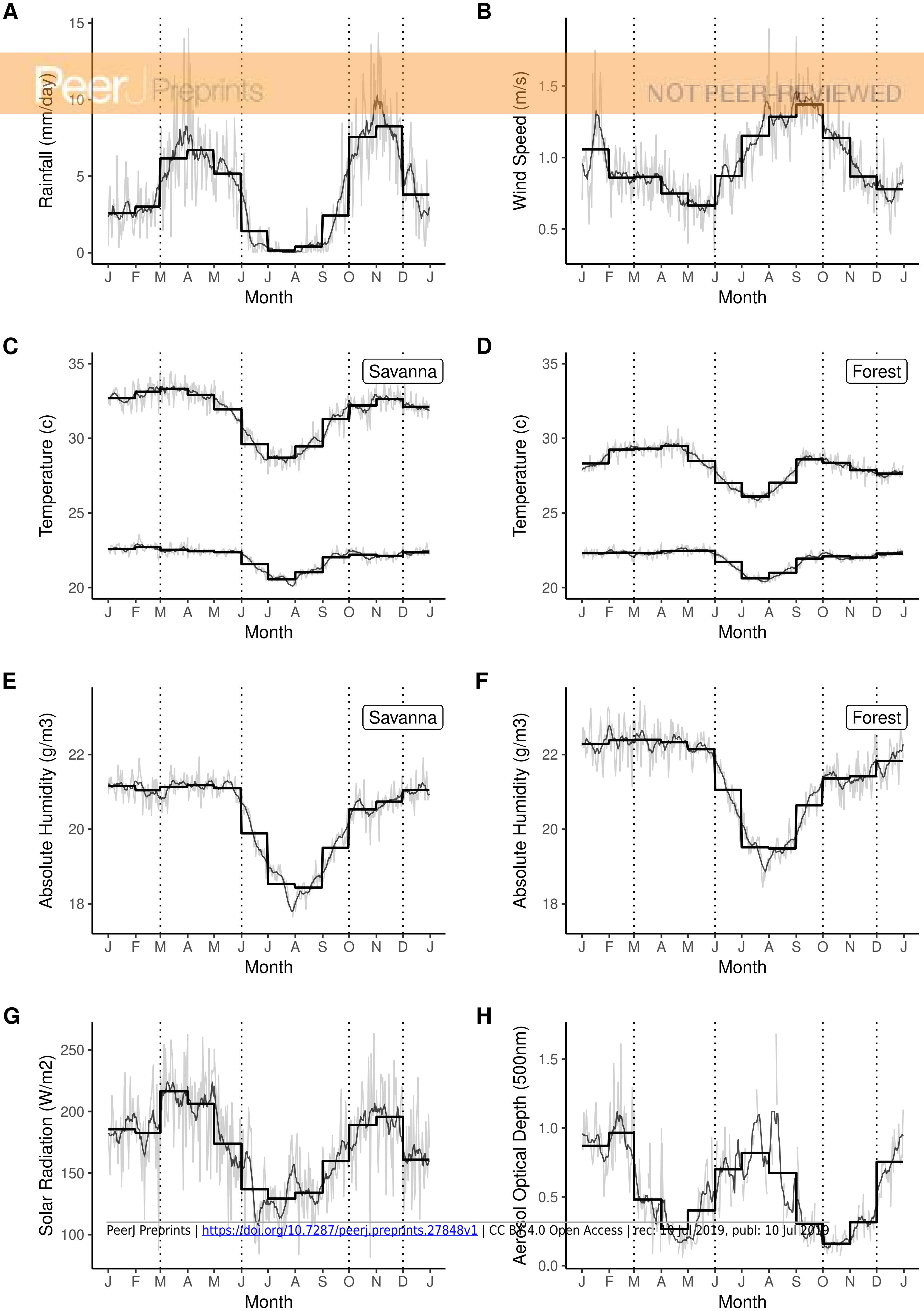
A
Rainfall (mm/day)
Month
B
Wind Speed (m/s)
Month
C
Savanna
Temperature (c)
Month
D
Forest
Temperature (c)
Month
E
Savanna
Absolute Humidity (g/m3)
Month
F
Forest
Absolute Humidity (g/m3)
Month
G
Solar Radiation (W/m2)
Month
H
Aerosol Optical Depth (500nm)
Month
J F M A M J J A S O N D J

Figure 3 (on next page)

Inter-annual variation, long-term trends and periodicity for rainfall and temperature at Lopé NP, Gabon.

(A) The grey lines indicate inter-annual variation and the black line indicates the long-term trend for total annual rainfall (1984-2018) derived from a generalised linear model (family = poisson). (B) The grey dots indicate raw daily data summarised to monthly means and the black line indicates the long-term trend for minimum daily temperature (1984-2018) derived from a linear mixed model. (C, D) Wavelet transforms of the monthly time-series for total monthly rainfall and mean minimum daily temperature. The faded region indicates the “cone of influence” where end effects made the data unreliable. The colour indicates the power of the cycle at each time period, red= high power and blue = low power. Bold black lines indicate cycles with significant power (Chi-sq test). (E, F) Extracted wavelet components for the biannual, annual and multi-annual (mean of 2-4 years) periods from the wavelet transforms adjusted for edge effects.

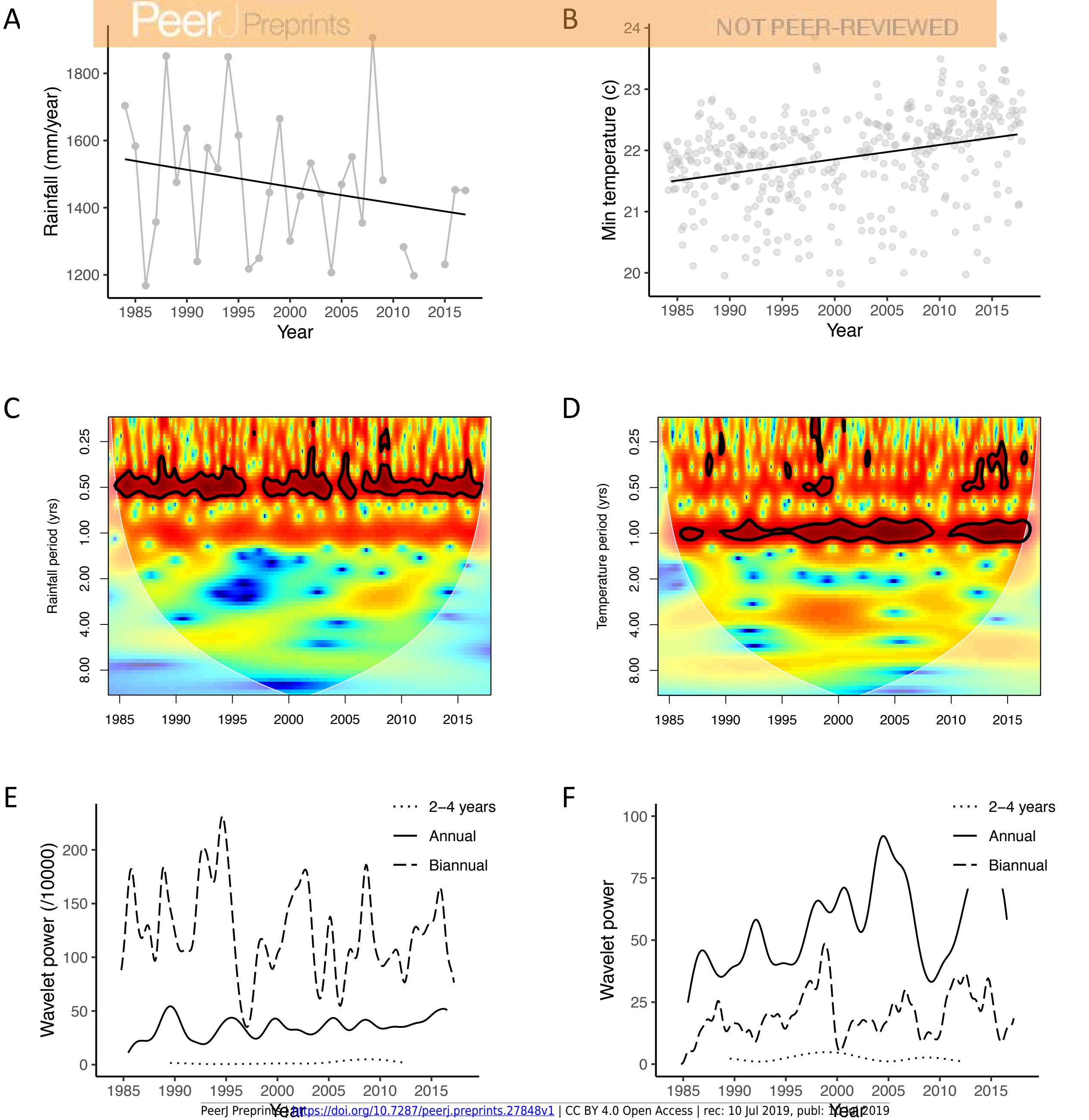

A
Rainfall (mm/year)
1800
1600
1400
1200
1985
1990
1995
2000
2005
2010
2015
Year
B
Min temperature (c)
24
23
22
21
20
Year
C
Rainfall period (yrs)
0.25
0.50
1.00
2.00
4.00
8.00
D
Temperature period (yrs)
E
Wavelet power (/10000)
200
150
100
50
0
2–4 years
Annual
Biannual
Year
F
Wavelet power
100
75
50
25
0
Year

Figure 4(on next page)

Oceanic influences on rainfall and temperature at Lopé NP, Gabon.

(A) Standardised effect sizes for significant correlations between oceanic indices (NATL = northern tropical Atlantic SST, SATL= southern equatorial Atlantic SST, MEI = Multivariate ENSO Index, IOD = Indian Ocean Dipole) derived from the best models for oceanic influences on total monthly rainfall (generalised linear mixed model, family = poisson) and monthly mean minimum temperature (linear mixed model). The colour of the dot indicates the direction of the correlation (blue= positive, red=negative). The size of the circle indicates the relative size of the effect and the transparency of the circle indicates the uncertainty (low transparency = low T/Z value, high transparency = high T/Z value). (B-F) The points indicate raw data summarised to seasonal means and the lines indicate model predictions from the best models for oceanic influences on rainfall (generalised linear mixed model, family = poisson) and temperature (linear mixed model).

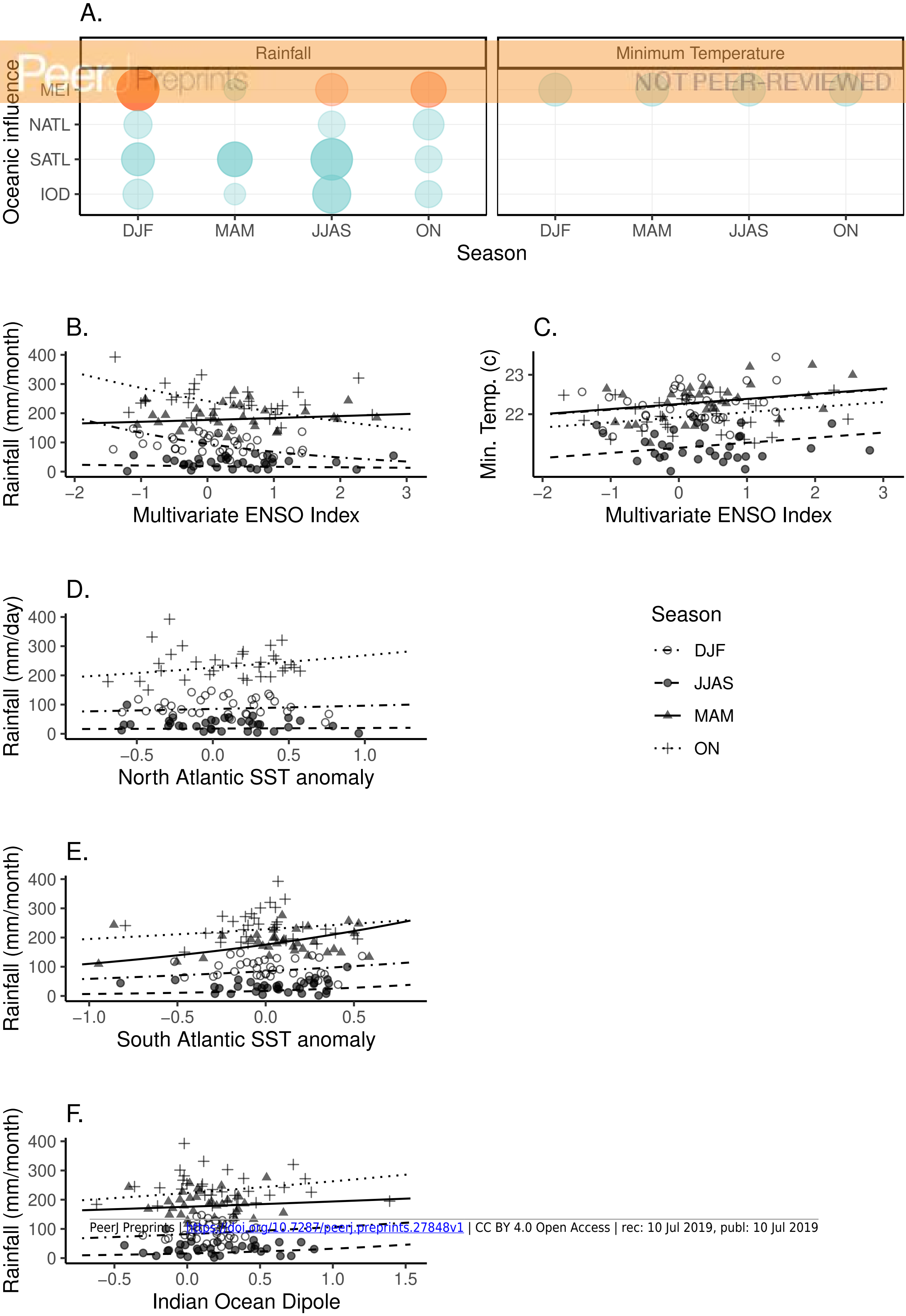

PeerJ Preprints | https://doi.org/10.7287/peerj.preprints.27848v1 | CC BY 4.0 Open Access | rec: 10 Jul 2019, publ: 10 Jul 2019

Table 1(on next page)

Major oceanic influences on rainfall in western equatorial Africa.

PeerJ Preprints | https://doi.org/10.7287/peerj.preprints.27848v1 | CC BY 4.0 Open Access | rec: 10 Jul 2019, publ: 10 Jul 2019

Study	Description	Ocean influences	
Preethi et al 2015.	Africa-wide; Satellite and gridded obs.; 1979-2010.	Pacific:	Canonical El Niño reduces rainfall Jan-Sep. El Niño Modoki increases rainfall Mar-May.
		Indian:	Positive relationship between SSTs and rainfall Jan-Feb. No relationship between IOD and rainfall.
Camberlin et al. 2001.	Sub-Sahara; Gridded obs.; 1951-1997.	Pacific:	El Niño negatively influences rainfall Apr-Jun.
		Atlantic:	South Atlantic SSTs positively influence rainfall Apr-Sep.
Balas et al. 2007.	WEA; Precipitation gauge dataset; 1950-1998.	Pacific:	El Niño negatively influences rainfall.
		Indian:	Weak positive relationship between SSTs and rainfall in all seasons except Mar-May when it is reversed.
		Atlantic:	Positive correlation between south Atlantic SSTs and rainfall Jun-Nov, negative influence Dec-Feb. Benguela coast influences rain Mar-May.
Todd & Washington 2004.	CEA and WEA; Gridded obs. and discharge data Feb-Apr; 1901-1998.	Pacific:	El Niño has weak negative influence on rainfall Feb-Apr.
		Atlantic:	North Atlantic Oscillation negatively influences rainfall Feb-Apr.
Otto et al. 2013.	CEA and WEA; Simulated data. Dry seasons only.	Pacific:	ENSO influences rainfall in dry seasons.
		Indian:	IOD negatively influences rainfall in dry seasons.
		Atlantic:	Warm tropical Atlantic SSTs enhance rain in dry seasons.
Nicholson & Dezfuli 2013; Dezfuli & Nicholson 2013.	WEA. Regionalised obs. Rainy seasons only.	Pacific:	El Niño reduces rainfall in rainy seasons.
		Indian:	Positive IOD modes associated with reduced rainfall in rainy seasons.
		Atlantic:	Warm tropical Atlantic SSTs enhance rainfall in rainy seasons. Strong correlation with Benguela coast from Oct-Dec

CEA = central equatorial Africa, WEA = western equatorial Africa, SST = sea surface temperatures, ENSO = El Niño Southern Oscillation, IOD = Indian Ocean Dipole.

Table 2(on next page)

Model comparisons to test for long-term trends in rainfall and minimum temperature at Lopé NP, Gabon (1984-2018).

We used a generalised linear model (family = poisson) for total annual rainfall and a linear mixed model for minimum daily temperature. Year and Day of Year were included as random intercepts in the mixed model.

Response	Model	Predictors	AIC	DF
Rainfall	Long-term change	Year	1051.9	2
	No long-term change	Intercept only	1097.7	1
Temperature	Long-term change	Year	22573.0	5
	No long-term change	Intercept only	22586.2	4

AIC = Akaike Information Criterion, DF = Degrees of Freedom.

PeerJ Preprints | https://doi.org/10.7287/peerj.preprints.27848v1 | CC BY 4.0 Open Access | rec: 10 Jul 2019, publ: 10 Jul 2019

Table 3 (on next page)

Model comparisons to test for long-term trends in rainfall and minimum temperature varying by season at Lopé NP, Gabon (1984-2018).

We used a generalised linear mixed model (family = poisson) for daily rainfall and a linear mixed model for minimum daily temperature. Year and Day of Year were included as random intercepts in both mixed models.

PeerJ Preprints | https://doi.org/10.7287/peerj.preprints.27848v1 | CC BY 4.0 Open Access | rec: 10 Jul 2019, publ: 10 Jul 2019

Response	Model	Predictors	AIC	DF
Rainfall	Long-term change varying by season	Year * Season	151398.4	10
	Long-term change not varying by season	Year + Season	151615.0	7
Temperature	Long-term change varying by season	Year * Season	22237.7	11
	Long-term change not varying by season	Year + Season	22251.5	8

AIC = Akaike Information Criterion, DF = Degrees of Freedom.

Table 4(on next page)

Outputs from the best models for long-term trends in rainfall and minimum daily temperature varying by season at Lopé NP, Gabon (1984-2018).

Estimates derived from a generalised linear mixed model (family = poisson) for daily rainfall and a linear mixed model for minimum daily temperature. Year and Day of Year were included as random effects in both mixed models. Asterisks indicate estimates for which the 95% confidence interval does not overlap zero.

Response	Predictor	Estimate	SE	T/Z Value	95% CI	
Rainfall	DJF	0.69	0.12	5.62	0.45,0.93	*
	JJAS	-0.02	0.11	-0.23	-0.24,0.19	
	MAM	1.12	0.11	10.01	0.9,1.34	*
	ON	0.72	0.13	5.48	0.46,0.98	*
	Year: DJF	0.02	0.03	0.92	-0.03,0.08	
	Year: JJAS	-0.25	0.03	-8.75	-0.31,-0.19	*
	Year: MAM	-0.06	0.03	-2.36	-0.11,-0.01	*
	Year: ON	-0.03	0.03	-1.28	-0.08,0.02	
Temperature	DJF	22.28	0.06	371.77	22.16,22.4	*
	JJAS	21.22	0.06	379.56	21.11,21.33	*
	MAM	22.31	0.06	375.03	22.19,22.43	*
	ON	21.95	0.07	329.92	21.82,22.08	*
	Year: DJF	0.28	0.05	6.10	0.19,0.38	*
	Year: JJAS	0.16	0.05	3.43	0.07,0.25	*
	Year: MAM	0.24	0.05	5.09	0.15,0.33	*
	Year: ON	0.30	0.05	6.06	0.2,0.39	*

SE = Standard Error, CI = Confidence Interval

Table 5(on next page)

Model comparisons to test for oceanic influences on rainfall and minimum temperature at Lopé NP, Gabon (1984-2018).

We used a generalised linear mixed model (family = poisson) for monthly rainfall and a linear mixed model for monthly mean minimum daily temperature. Year and Month were included as random effects in both mixed models.

Response	Predictors	AIC	DF
Rainfall	Season + NATL: Season + SATL: Season + MEI: Season + IOD: Season + Year: Season	12253.9	26
	Season + NATL: Season + SATL: Season + MEI: Season + IOD + Year: Season	12346.4	23
	Season + NATL: Season + SATL: Season + MEI + IOD: Season + Year: Season	12867.6	23
	Season + NATL: Season + SATL + MEI: Season + IOD: Season + Year: Season	12396.5	23
	Season + NATL + SATL: Season + MEI: Season + IOD: Season + Year: Season	12269.7	23
Temperature	Season + NATL: Season + SATL: Season + MEI: Season + IOD: Season + Year: Season	500.4	27
	Season + NATL: Season + SATL: Season + MEI: Season + IOD + Year: Season	484.0	24
	Season + NATL: Season + SATL: Season + MEI: Season + Year: Season	476.8	23
	Season + NATL: Season + SATL: Season + MEI + Year: Season	466.1	20
	Season + NATL: Season + SATL: Season + Year: Season	473.2	19
	Season + NATL: Season + SATL + MEI + Year: Season	456.0	17
	Season + NATL: Season + MEI + Year: Season	449.3	16
	Season + NATL + MEI + Year: Season	435.2	13
	Season + MEI + Year: Season	432.9	12

AIC = Akaike Information Criterion, DF = Degrees of Freedom, MEI = Multivariate ENSO Index, NATL = Tropical North Atlantic, SATL = Tropical South Atlantic, IOD = Indian Ocean Dipole

PeerJ Preprints | https://doi.org/10.7287/peerj.preprints.27848v1 | CC BY 4.0 Open Access | rec: 10 Jul 2019, publ: 10 Jul 2019

Table 6(on next page)

Outputs from the best model for oceanic influences on rainfall at Lopé NP, Gabon (1984-2018).

Estimates derived from a modified generalized linear mixed model (family = poisson) on monthly rainfall with the global intercept temporarily removed to allow direct comparisons between the estimates for each season. Asterisks indicate estimates for which the 95% confidence interval does not overlap zero.

PeerJ Preprints | https://doi.org/10.7287/peerj.preprints.27848v1 | CC BY 4.0 Open Access | rec: 10 Jul 2019, publ: 10 Jul 2019

Predictor	Estimate	SE	Z Value	95% CI	
DJF	4.45	0.37	11.89	3.72,5.19	*
JJAS	2.89	0.33	8.88	2.25,3.53	*
MAM	5.19	0.37	13.85	4.45,5.92	*
ON	5.44	0.46	11.87	4.54,6.33	*
MEI: DJF	-0.32	0.01	-24.73	-0.35,-0.3	*
MEI: JJAS	-0.11	0.02	-5.24	-0.15,-0.07	*
MEI: MAM	0.03	0.01	3.04	0.01,0.06	*
MEI: ON	-0.16	0.01	-11.33	-0.19,-0.13	*
NATL: DJF	0.06	0.02	4.18	0.03,0.09	*
NATL: JJAS	0.05	0.02	2.41	0.01,0.1	*
NATL: MAM	0.01	0.01	0.65	-0.02,0.03	
NATL: ON	0.09	0.02	4.89	0.05,0.12	*
SATL: DJF	0.12	0.01	10.50	0.1,0.14	*
SATL: JJAS	0.31	0.02	15.62	0.27,0.35	*
SATL: MAM	0.15	0.01	15.48	0.13,0.17	*
SATL: ON	0.05	0.01	4.11	0.03,0.08	*
IOD: DJF	0.08	0.02	4.70	0.05,0.12	*
IOD: JJAS	0.22	0.02	12.31	0.19,0.26	*
IOD: MAM	0.03	0.01	2.56	0.01,0.05	*
IOD: ON	0.05	0.01	4.73	0.03,0.07	*
Year: DJF	-0.04	0.04	-1.21	-0.11,0.03	
Year: JJAS	-0.34	0.04	-8.69	-0.42,-0.27	*
Year: MAM	-0.09	0.04	-2.55	-0.16,-0.02	*
Year: ON	-0.09	0.04	-2.37	-0.16,-0.02	*

SE = Standard Error, CI = Confidence Interval, MEI = Multivariate ENSO Index, NATL = Tropical North Atlantic, SATL = Tropical South Atlantic, IOD = Indian Ocean Dipole

PeerJ Preprints | https://doi.org/10.7287/peerj.preprints.27848v1 | CC BY 4.0 Open Access | rec: 10 Jul 2019, publ: 10 Jul 2019

Table 7(on next page)

Outputs from the best model for oceanic influences on temperature at Lopé NP, Gabon (1984-2018).

Estimates are derived from a linear mixed model on monthly mean minimum daily temperature with the global intercept temporarily removed to allow direct comparison between the estimates for each season. Asterisks indicate estimates for which the 95% confidence interval does not overlap zero.

PeerJ Preprints | https://doi.org/10.7287/peerj.preprints.27848v1 | CC BY 4.0 Open Access | rec: 10 Jul 2019, publ: 10 Jul 2019

Predictor	Estimate	SE	T Value	95% CI	
DJF	22.28	0.21	104.85	21.87,22.7	*
JJAS	21.19	0.19	114.51	20.82,21.55	*
MAM	22.3	0.21	105.03	21.88,22.71	*
ON	21.96	0.26	84.92	21.45,22.47	*
MEI	0.12	0.03	4.60	0.07,0.18	*
Year: DJF	0.31	0.06	5.56	0.2,0.41	*
Year: JJAS	0.16	0.05	3.05	0.06,0.26	*
Year: MAM	0.25	0.05	4.63	0.14,0.36	*
Year: ON	0.31	0.06	5.04	0.19,0.43	*

SE = Standard Error, CI = Confidence Interval, MEI = Multivariate ENSO Index

PeerJ Preprints | https://doi.org/10.7287/peerj.preprints.27848v1 | CC BY 4.0 Open Access | rec: 10 Jul 2019, publ: 10 Jul 2019